5-2022

The Design of a Efficient Production and Purification of Fibroblast Growth Factor 2

Mandeep Kaur
University of Arkansas, Fayetteville

The Design of a Efficient Production and Purification of Fibroblast Growth Factor 2

A thesis submitted in partial fulfillment of the honors requirement

for the degree of Bachelor of Science in Chemistry

with a Biochemistry Concentration

By

Mandeep Kaur

May 2022

University of Arkansas

Fayetteville, AR

Acknowledgements

I would like to thank Dr.Kumar, the Kumar Lab group, graduate students – Ryan Layes and Shivakumar Sonnailia, and the senior undergraduate students in the Kumar Lab. I would also like to thank University of Arkansas Honor's Research Grant that I was awarded in Fall 2020.

Table of Contents

Abstract

Chronic wounds pose a major problem in the United States with an estimate of twenty-five million dollars a year spent on associated treatments. Growth factors can be used as a potential treatment for chronic wounds since they promote cell proliferation and angiogenesis. This study employs one specific growth factor, fibroblast growth factor 2 (FGF2) so that it could potentially be used in future treatment. Wild-type FGF2 is thermally unstable, and it has a mean elimination time of 7.6 hours. This study attempted to improve upon its stability through a mutation on the heparin binding loop. The mutation performed was K134E. This mutation decreased the number of electrostatic interactions present on the heparin-binding loop.

FGF2 was first be attained through the large-scale expression of glutathione-S-transferase-fibroblast growth factor 2 (GST-FGF2). GST-tag was then cleaved from GST-FGF2 by thrombin digestion. The stability and structure were studied through differential scanning calorimetry, circular dichroism, and florescence. This process is a low-cost method since GST-FGF2 was purified from an *E. coli* culture containing the mutant plasmid

Even though both wild-type and mutant protein were successfully purified at least once, there was not enough protein purified for neither to conduct all characterization studies. A purification procedure was established, and it is possible that the mutant has greater thermal stability than the wild-type but further studies are still needed to make a definitive conclusion.

Introduction

Much like all relationships, communication is key for the human body. The body has several molecules that allow for cell signaling such as syntactic transmission, hormones, ligands, or the extracellular matrix. (1) These signals are vital since they allow the cell to produce an intercellular response that is appropriate to their environment.

One type of cell-signaling molecules are growth factors which includes several protein families. Each factor is associated with different types of cells and activity. Although all growth factors are associated with the proliferation of cells and target tissues, each growth factors binds to specific receptors on a cells' surface to elicit desired responses (2).

However, within each family of growth factors, they can be further differentiated. Fibroblast growth factors (FGF) are a family (*Figure 1)* of 23 structurally related proteins, which can be further divided into six-subfamilies in humans (3) (4). All FGFs have a molecular weight between 17 and 34 kilodalton (kDa) (3). The function of the FGF varies; different members have roles varying from embryonic development, maintenance of adult organ systems, tissue regeneration, wound repair, and hematopoiesis (3). Interestingly, mutations within FGF have been found linked to disease. For example, the

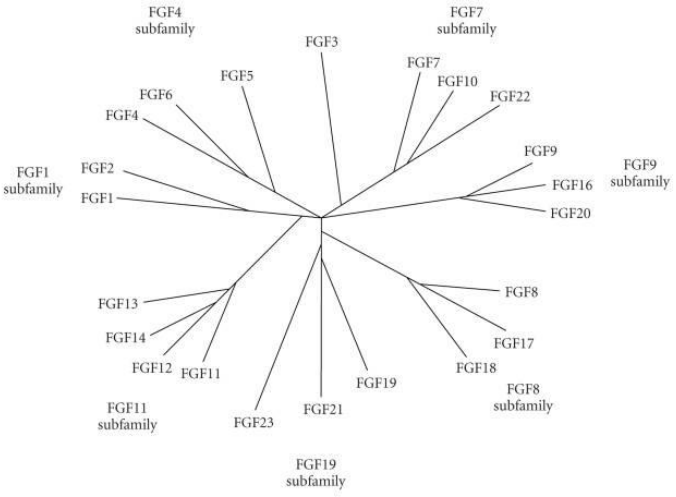

Figure 1: Family diagram of human FGF and relations within the family (Yun 2010)

loss of FGF3 is seen linked to hereditary deafness and degradation of FGF8 leads to Kallman's disease which is a developmental disorder that involves anosmia and hypogonadism (3). This link between mutation and disease with FGFs only further signifies the importance of FGFs in the human body.

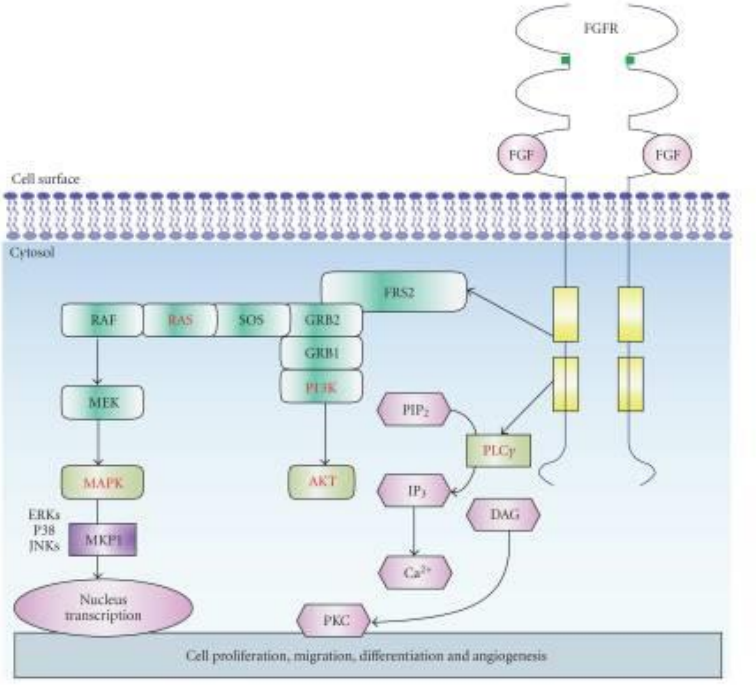

Figure 2: The signaling pathway for each of the three pathways of FGF2 (Yun 2010)

FGF stimulates cell-signaling functions in the human body since FGF activates upon binding and dimerization with fibroblast growth factor receptors (FGFRs) (5). FGFR is a family of four genes that encode receptors that consists of three extracellular immunoglobulin-like domains, a single-pass transmembrane, and a cytoplasmic tyrosine kinase domain (6). FGF can bind to FGFR through a dimer conjoined by heparin sulfate proteoglycans (HPSG) that facilitates the FGF/FGFR dimer (7). On the molecular level, the typical FGF gene has three coding exons with one exon that contains the initiation methionine (8). There are typically three pathways that describe the signal of FGF (*Figure 2)* – RAS/MAP kinase pathway, PI3 kinase/AKT pathway, and PLC γ (4). This study focuses on one specific protein within the FGF family: fibroblast growth factor 2 (FGF2).

Fibroblast Growth Factor 2 –(FGF2)

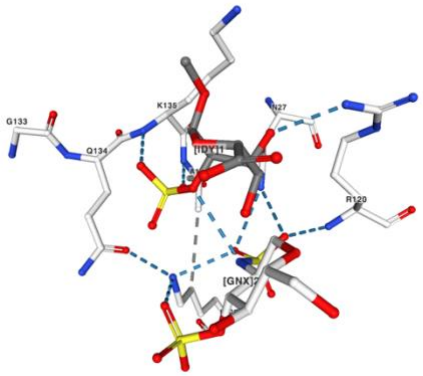

Figure 3: Crystal Structure of FGF2 (Yi-Ching 2014)

FGF2 (*Figure 3)* is an 18 kDa protein that promotes a large variety of processes which include cell proliferation, migration, vasculogenesis, angiogenesis, cell differentiation, and stem cell renewal (9).

All FGFs have a homologous trefoil core consisting of 12 anti-parallel beta strands. It is variations in the amino acid sequences at the opposite terminal regions that account for the biological differences (10). FGF2 also has these 12 antiparallel beta strands that are in core region of the protein (9). FGF2 is slightly different than other proteins in the FGF family as it lacks a transient signal peptide. FGF2 does not have a defined mechanism for secretion that been characterized besides its release from dead or injured cells (11). This indicates that FGF2 may play a larger role in healing and repairing rather than normal bodily functions which is different than other proteins in the FGF family.

FGF2 is partially able to play this role due to its binding affinity with heparin (8). Heparin sulfate is a sulfated linear polysaccharide with alternating 1→ 4 linked with alpha-D glucosamine and beta-D-glucuronic acid (12). FGF2 combines with HSPG which help stabilize FGF and HPSG binding is a vital component of FGF signaling *in vivo* (13). FGF2 interacts with heparin through the N-sulfonated glucosamine (GlcN) and the 2-O-sulfonated iduronic acid (IdoA2S). The 6-sulfonated groups of GlcN are required

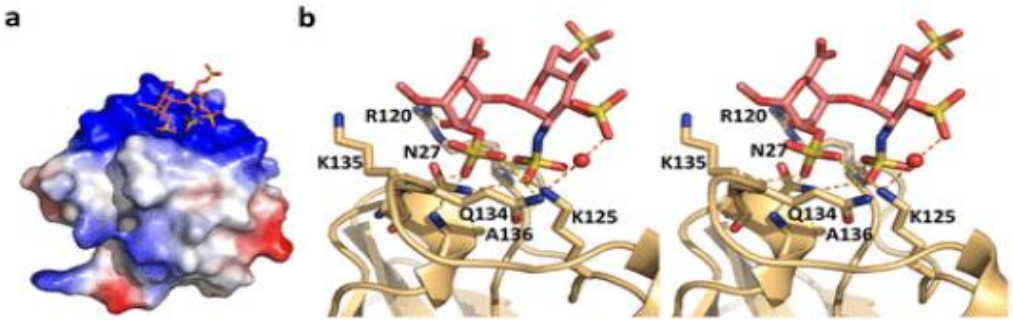

Figure 4: Interactions of FGF2 with Heparin (YI Ci 2014)

for FGF2 receptor activation (14). *Figure 4* shows this interaction between heparin and FGF2 in more detail. In *Figure 4*, the electrostatic potential is mapped onto the surface of FGF2 with positive electrostatic potential showing the HS binding site as shown in pink. Furthermore, beta strand 10 and beta strand 11 are the strands that form the primary heparin binding site (7). This allows for the formation of the tertiary FGF2: FGFR: heparin complex. It has been shown that interaction between FGF2 and HSPG increases the binding affinity of FGF2 for FGFR. This increased binding affinity leads to an increased cellular response (15). These proliferative qualities of FGF2 combined with its affinity for heparin binding potentially makes it a useful wound healing agent.

Significance of Study

Finding possible treatments for wound repair is essential since chronic wounds are a major problem in the United States. Each year, an average of 6.5 million patients are affected with wound care costs that end up greater than twenty-five million dollars (5). Chronic wounds are commonly comorbid in obese and diabetic patients. More than one million diabetic patients worldwide lose a lower limb from an infection that resulted from a foot ulcer (16). Pressure ulcers are also very common with 72% of all patients over the age of 65 eventually developing one (17).

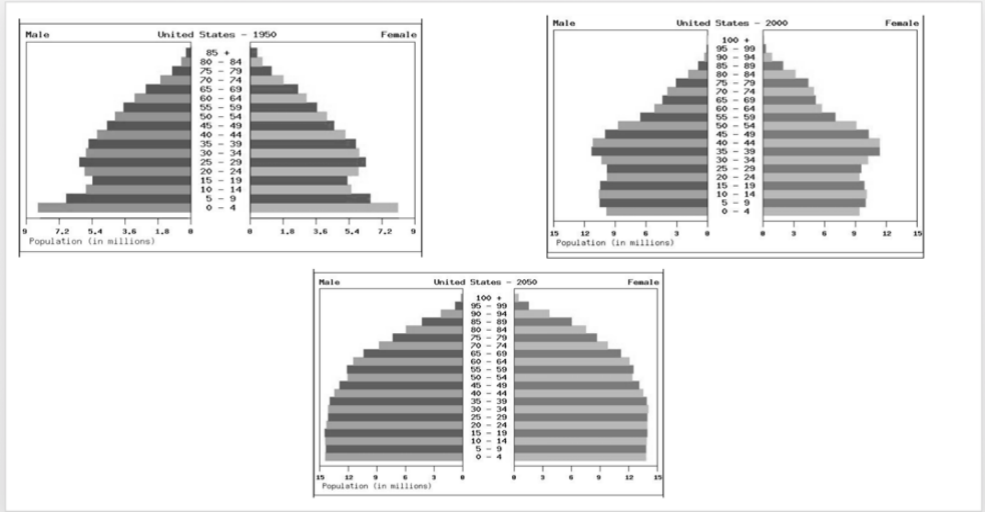

Figure 5: Aging Population of the United States (Shrestha 2011)

The need to augment wound repair is further demonstrated by the aging population of the United States. *Figure 5* shows the aging population of the United States as times progresses throughout the past century (18). In 1950, the median age of the United States was 30.4. However, by 2050, the median age of the United States is projected to be 35.3 years (18). While this may not seem like a major change, it is projected about 12.4 % of the US population or 35.1 million people will be older than 65 years old (18). Since age and pressure wounds are closely correlated, it is essential that better treatments are found so elderly people receive the best treatment.

FGF2 has already been manipulated to provide treatment for chronic wounds as seen through the development of Regranex. This growth factor containing gel is supposed to aid in the healing of chronic wounds. However, the functionality and activity of FGF2 in terms of wound healing has not been addressed (19). Further research needs to be done to evaluate the effectiveness of FGF2 in wound healing.

Another example of FGF2 being used as a wound healing agent was observed in study in which 16 patients were treated with a sustained-release FGF2 loaded collagen/gelatin sponge. Favorable outcomes were observed for all patients that helped prevent possibly invasive surgical techniques (20). However, this would not be reproducible in a standard clinical setting due to the instability of the protein in solution. For this study, multiple high doses of FGF2 were administered daily to compensate for the quick loss of biological function of FGF2 at wound sites (20).

The key to finding an effective treatment is to improve the stability of FGF2. FGF2 has a mean apparent terminal elimination of 7.6 hours (21). Currently, unmodified FGF2 is inactive after standard storage conditions. Exposure to refrigeration for seven days without modifications to the stability results in an inactive protein. This indicates that wild-type FGF2 cannot be used in a clinical setting (21). Furthermore, FGF2 has been seen to lose over 50% of its functionality after 46 minutes in storage at 25˚C (20). A secondary issue is the high cost associated with current models of deriving FGF2 (21). To combat these issues, this study involves deriving a technique for the efficient purification of FGF2 and mutating the protein so that it has greater stability.

Site-Directed Mutagenesis

The mutation performed was K134E on FGF2 as shown in *Figure 6*. *Figure 6* displays the pairwise alignment of the sequence with the wildtype sequence on the top and the mutated sequence on the bottom

```
   1 MAAGSITTLPALPEDGGSGAFPPGHFKDPKRLYCKNGGFFLRIHPDGRVD     50
     |||||||||||||||||||||||||||||||||||||||||||||||||||
   1 MAAGSITTLPALPEDGGSGAFPPGHFKDPKRLYCKNGGFFLRIHPDGRVD     50

  51 GVREKSDPHIKLQLQAEERGVVSIKGVCANRYLAMKEDGRLLASKCVTDE    100
     |||||||||||||||||||||||||||||||||||||||||||||||||||
  51 GVREKSDPHIKLQLQAEERGVVSIKGVCANRYLAMKEDGRLLASKCVTDE    100

 101 CFFFERLESNNYNTYRSRKYTSWYVALKRTGQYKLGSKTGPGQKAILFLP    150
     |||||||||||||||||||||||||||||||:|||||||||||||||||
 101 CFFFERLESNNYNTYRSRKYTSWYVALKRTGQYELGSKTGPGQKAILFLP    150

 151 MSAKS    155
     |||||
 151 MSAKS    155
```

Figure 6: Pairwise alignment of sequence with wtFGF2 sequence on top and K134E sequence on bottom

This mutation involves taking a positively charged amino acid, Lysine (K), and mutating into glutamic acid (E) which is a negatively charged amino acid. This mutation is done to lower the number of electrostatic interactions present in the heparin binding loop since K134 is present in the heparin binding loop (7). Since heparin stabilizes FGF2, having decreased electrostatic interactions in the heparin binding loop will likely lead to a more stable FGF2-heparin complex.

Furthermore, a similar mutation has been performed on FGF1 that resulted in the increased thermal and chemical stability of FGF1. A R136E mutation was performed on FGF1 which led to increased chemical and thermal stability (22). In FGF2, K134 is considered homologous to R136 in FGF1. Hence, the mutation performed was K134E.

Materials and Methods

The following techniques were used to determine the effects of the K134E mutation on the FGF2 structure. Firstly, the desired mutants are over-expressed and purified. The methodology and characterization studies employed are listed below.

Overexpression and Purification of FGF2: Initial steps of the research included bacterial transformation, large scale expression, and purification of GST-FGF2. Bacterial transformation was firstly done to create a glycerol stock containing an *E. coli* culture that had the mutant plasmid. Large scale separation was than conducted using β- d-1-thiogalactopyranoside (IPTG) and it was grown in liquid Luris-Bertani (LB) broth. Since the plasmid is added after the lac-operon, IPTG can act upon this and overexpress the desired plasmid. Purification was done through a GSH-sepharose column in a phosphate buffer containing 10 mM phosphate, 150 mM NaCl, 25 mM ammonium sulfate, and 10% glycerol *(Buffer 1)*. Afterwards, a SDS-PAGE was ran to verify successful purification of FGF2.

Thrombin Cleavage: To separate GST from GST-FGF2, thrombin cleavage was performed. The same column where protein loading was performed, the column was incubated with thrombin and left to shake overnight. Afterwards, purification was run again elute FGF2 from the column while GST remained bound to the resin. To remove GST from the column, a 20 mM GSH buffer was ran through after FGF2 elution. An SDS-PAGE was run on both samples to see whether the purification was successful or not.

Florescence Spectroscopy: By using the change in fluorescence emission profile of FGF2, the proper activity of FGF2 after purification was confirmed.

Thermal denaturation: Thermal denaturation reveals how temperature affects the structure of FGF2. This is through the JASCO-1500 spectrofluorometer by collecting data of 0.5µM protein in a 10mM phosphate buffer for 5 minutes over a set temperature range.

Chemical denaturation: For chemical denaturation, urea and guanidium hydrochloride are used to induce protein denaturation. This process was monitored by using JACSO-1500 that uses intrinsic fluorescence emission. This information shows how stable the protein is in the presence of chemical denaturants.

Bioactivity: Bioactivity data is observed using 3T3 fibroblast cells grown in Dulbecco's Modified Eagle Medium (DMEM) supplemented with 10% fetal bovine serum (FBS). To monitor the rate of proliferation, there was prior adaptation of the medium before the inoculation with the protein samples.

Differential Scanning Calorimetry (DSC): This scan reveals the amount of energy required to increase 1 mol of protein by 1 K. The peak of this curve shows the melting temperature of both the mutant and wild type protein.

Circular Dichroism (CD) - CD was ran to ensure that the protein had proper secondary structure and folding. This ensures that there is no aggregation present in the protein that could limit its functionality and lead to denaturation.

Trypsin Digestion: Trypsin digestion helped to determine the structural rigidity of the wild-type and mutant protein of FGF2. To view this, time dependent digestion was performed. The results were assessed using an SDS-PAGE. The intensity of bands help reveals the structure and rigidity by comparing it to the control bands that have only protein and only trypsin.

Results

The pellets from large-scale expression were achieved for both the wild-type and mutant and were stored in a -20˚C cooler until they was ready for use. Before purifying, the bacterial pellet was sonicated to lyse cells and release proteins. For both wild-type and mutant, the purification took two days. All samples were kept on ice to prevent thermal denaturation while purifying. The first day, the protein was loaded onto the column. Then, thrombin was added to cleave the disulfide bond between GST and FGF2. The next day, FGF2 was eluted using *Buffer 1.*

Figure 7 displays the purification curves from day one and day two of the purification process of wt-GST-FGF2 through the GSH-sepharose column.

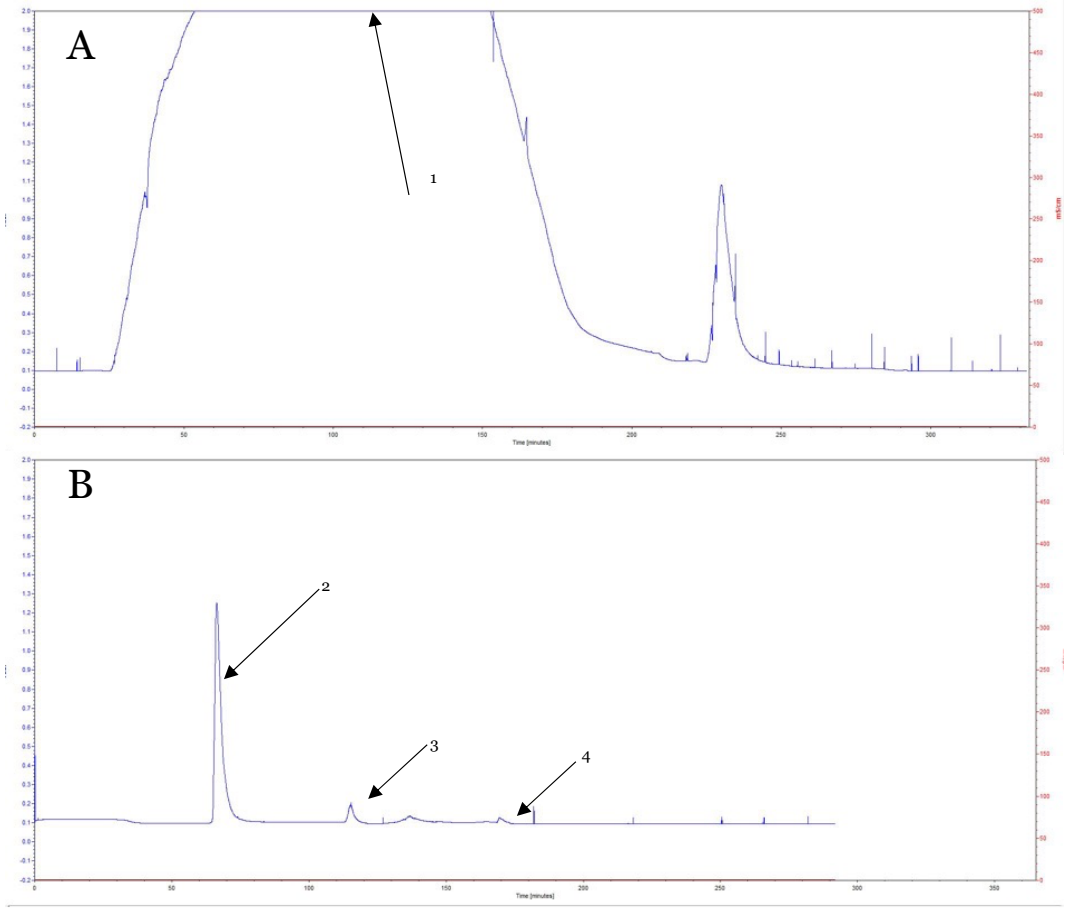

Figure 7: Purification profiles from purifying wt-GST-FGF2 via GSH-sepharose column.

***Graph A**; Day 1 purification profile before thrombin cleavage,*

***Peak 1:** Flowthrough peak from loading supernatant containing GST-FGF2 onto column*

***Graph B**; Day 2 purification profile after thrombin cleavage*

***Peak 2:** Peak while eluting wtFGF2 using a 10 mM phosphate and 20% glycerol buffer (pH:7.2) containing 150 mM NaCl*

***Peak 3:** Peak while eluting GST using 20 mM GSH buffer*

***Peak 4:** Peak eluting any additional containments left in the column using a 10 mM urea buffer*

Figure 8 shows a SDS-PAGE run after purification using a GSH-sepharose of the wild-type pellet. Lane 5 shows successful elution of the wild-type protein. However, there were several containments as well in Lane 5 which were not desired. To remove contaminants and obtain pure wtFGF2, the impure protein solution was further purified using a heparin-sepharose column.

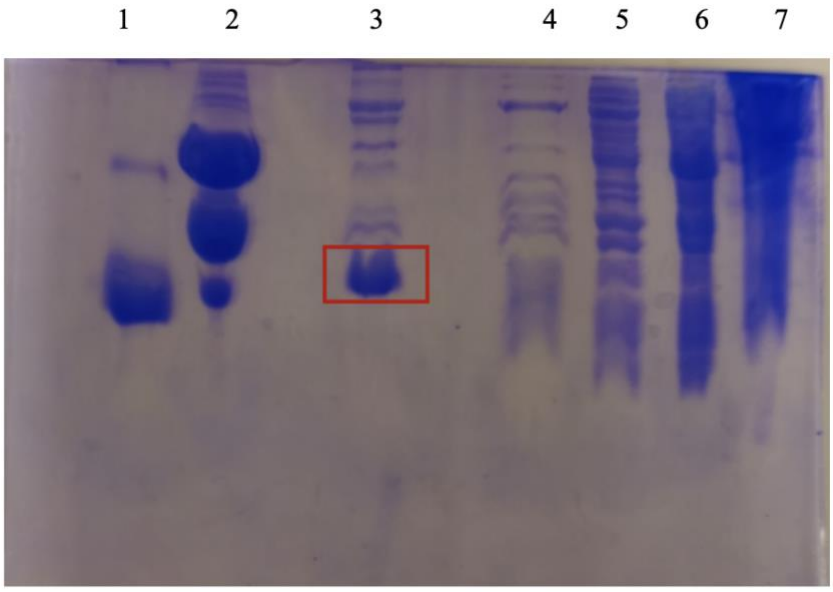

Figure 8: SDS-gel electrophoresis showing; ***Lane 1****- FGF1 marker;* ***Lane 2****- Flowthrough after thrombin cleavage in 20mM GSH buffer wash;* ***Lane 3****- wtFGF2 elution in 10 mM phosphate and 10 % glycerol buffer (pH:7.2) containing 150 mM NaCl;* ***Lane 4****- Flowthrough in 10 mM phosphate and 10% glycerol buffer (pH:7.2) containing 150 mM NaCl;* ***Lane 5*** *- Flowthrough in 10 mM phosphate and 10% glycerol buffer (pH:7.2) containing 150 mM NaCl;* ***Lane 6****- supernatant;* ***Lane 7****- pellet dissolved in 10 mM urea*

The red box indicates the band of interest of wtFGF2

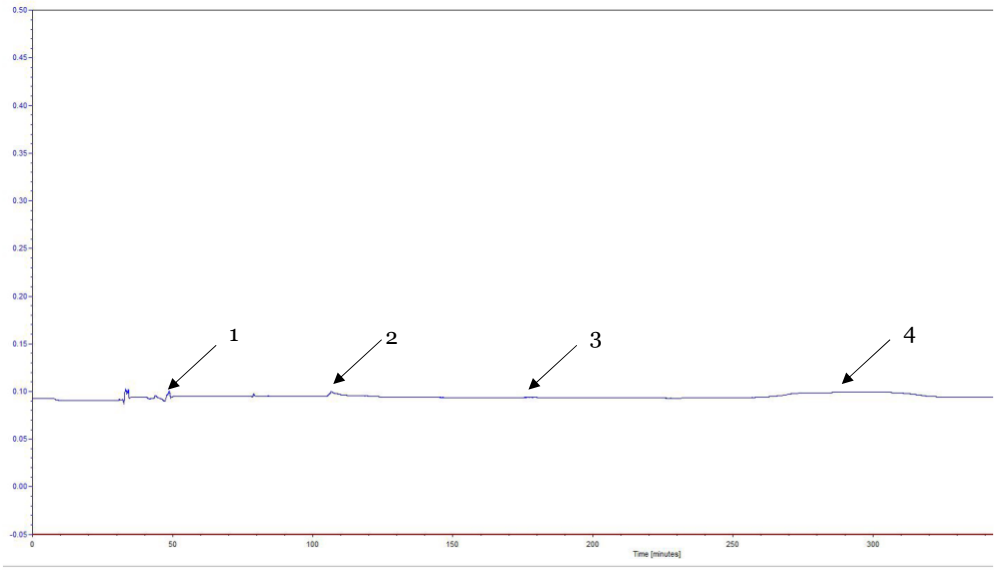

Figure 9: Purification profiles from purifying wt-GST-FGF2 via GSH-sepharose column.

Peak 1*- Flowthrough peak while loading wtFGF2 in 10 mM phosphate and 10% glycerol buffer (pH: 7.2) containing 150 NaCl onto column*

Peak 2*- Flowthrough peak while running 10 mM phosphate and 10% glycerol buffer (pH: 7.2) containing 300 NaCl*

Peak 3*- Flowthrough peak while running 10 mM phosphate and 10% glycerol buffer (pH: 7.2) containing 500 NaCl*

Peak 4*- wtFGF2 elution peak while running 10 mM phosphate and 10% glycerol buffer (pH: 7.2) containing 800 NaCl*

Figure 9 displays the purification profile of the wtFGF2 elution through a heparin-sepharose column. FGF2 was seen to elute when using a buffer containing a salt concentration of 800 mM.

Figure 10 shows an SDS-PAGE run after purification using the heparin-sepharose column. Lanes 4-7 show successful elution of the wtFGF2. This elution is pure since there are no additional bands. Lane 1 shows bands related to the containment bands proteins that were originally seen in the Lane 5 in *Figure 8*

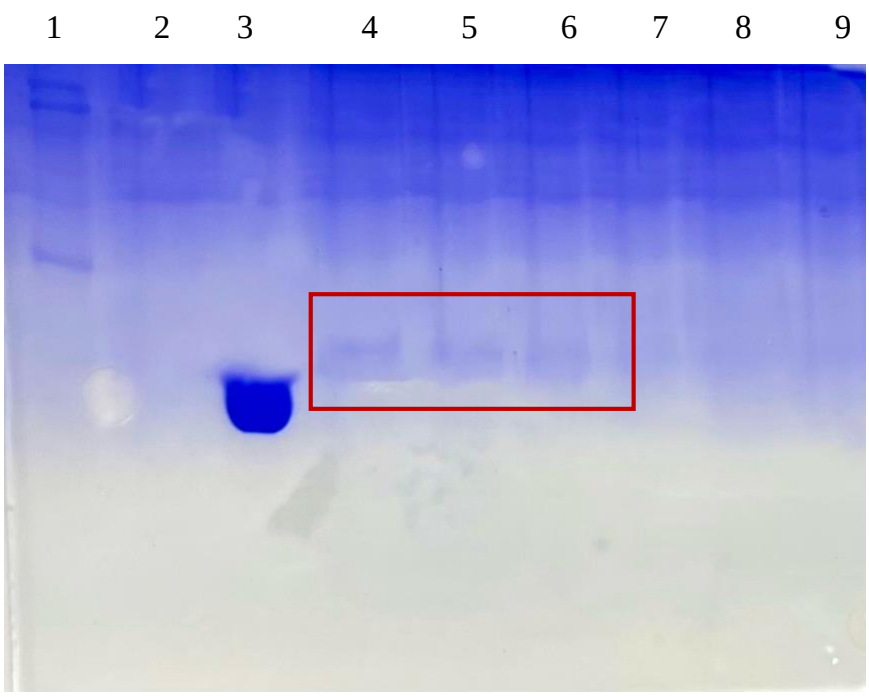

Figure 10- SDS-gel electrophoresis showing- ***Lane 1****, Flowthrough in 10 mM phosphate and 10 % glycerol buffer (pH:7.2) containing 150 mM NaCl;* ***Lane 2****, Flowthrough in 10 mM phosphate and 10 % glycerol buffer (pH:7.2) containing 500 mM NaCl;* ***Lane 3****, FGF1 markers;* ***Lane 4*** *wtFGF2 elution in 10 mM phosphate and 10 % glycerol buffer (pH:7.2) containing 800 mM NaCl;* ***Lane 5****, wtFGF2 elution in 10 mM phosphate and 10 % glycerol buffer (pH:7.2) containing 800 mM NaCl;* ***Lane 6****, wtFGF2 elution in 10 mM phosphate and 10 % glycerol buffer (pH:7.2) containing 800 mM NaCl;* ***Lane 7****, flowthrough in 10 mM phosphate and 10 % glycerol buffer (pH:7.2) containing 800 mM NaCl****;*** ***Lane 8****, flowthrough in 10 mM phosphate and 10 % glycerol buffer (pH:7.2) containing 800 mM NaCl;* ***Lane 9****, flowthrough in 10 mM phosphate and 10 % glycerol buffer (pH:7.2) containing 800 mM NaCl*

The red box indicates bands of wtFGF2

Similar results were seen with purification of the mutant pellet. The purification profile of K134E was similar to the purification profile of wtFGF2 as seen in *Figure 9.* The same procedure in terms of purification was followed as wtFGF2. SDS-PAGE (*Figure 11)* shows the results of the purification of the mutant using the GSH-sepharose column. Lane 5 shows that the protein was successfully eluted, but there were several containment bands as well.

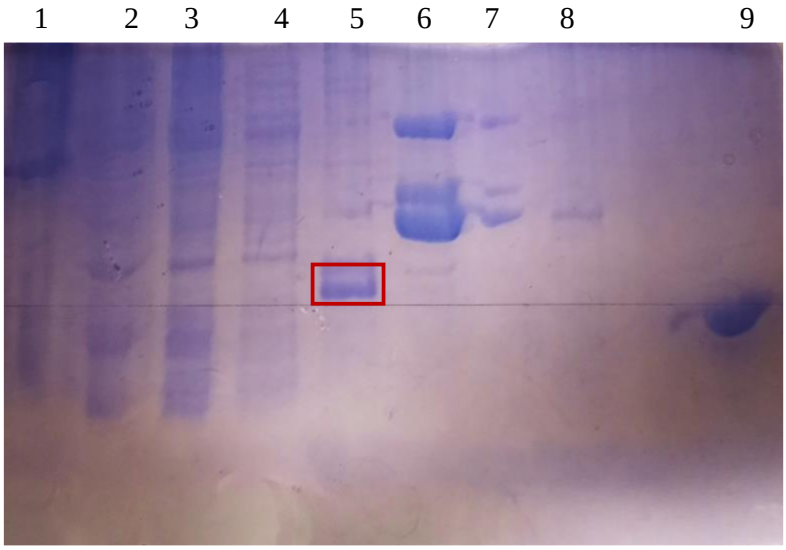

Figure 11: SDS-gel electrophoresis showing; ***Lane 1****- pellet dissolved in 10 mM urea;* ***Lane 2****- supernatant;* ***Lane 3****- Flowthrough in 10 mM phosphate and 10% glycerol buffer (pH:7.2) containing 150 mM NaCl;* ***Lane 4****- Flowthrough in 10 mM phosphate and 10% glycerol buffer (pH:7.2) containing 150 mM NaCl;* ***Lane 5****- K134E elution in 10 mM phosphate and 10% glycerol buffer (pH:7.2) containing 150 mM NaCl;* ***Lane 6*** *- Flowthrough after thrombin cleavage in 20mM GSH buffer wash;* ***Lane 7*** *Flowthrough after thrombin cleavage in 20mM GSH buffer wash;* ***Lane 8*** *– flowthrough column wash using 10 mM urea wash;* ***Lane 9****- FGF1 marker*

The red box indicates the band of interest of K134E

To clean up the protein, the mutant elution was then run through a heparin-sepharose column. The purification profile of K134E via the heparin-sepharose column was similar to wtFGF2 as seen in *Figure 9.* An SDS-PAGE as seen in *Figure 12* was then ran to verify purification. Lane 5 in *Figure 12* shows successful elution of the protein. Buffer-exchange was then run on the protein. The final concentration of the protein was 1 mg/mL, and the final volume was 1.8 mL.

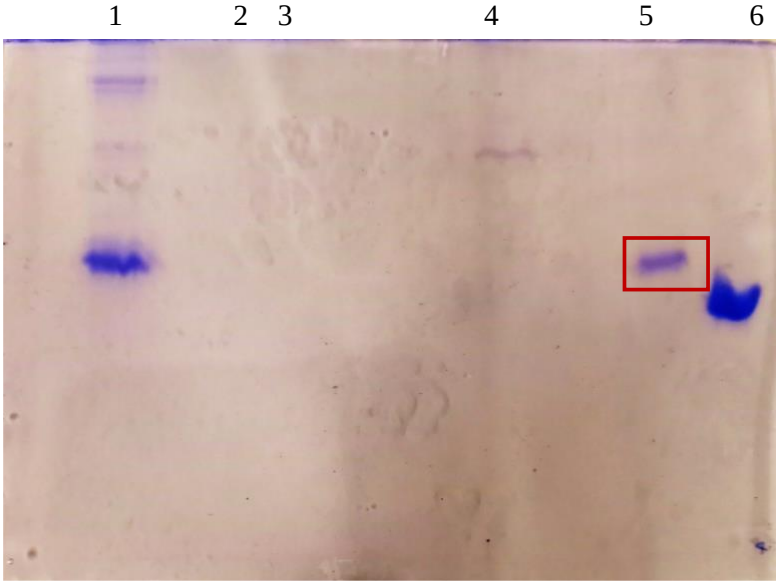

Figure 11- SDS-gel electrophoresis showing; ***Lane 1*** *– K134E elution in 10 mM phosphate and 10% glycerol buffer (pH:7.2) containing 150 mM NaCl achieved after GSH-Sepharose purification;* ***Lane 2****- Flowthrough in 10 mM phosphate and 10% glycerol buffer (pH:7.2) containing 150 mM NaCl;* ***Lane 3****- Flowthrough in 10 mM phosphate and 10% glycerol buffer (pH:7.2) containing 300 mM NaCl;* ***Lane 4*** *– Flowthrough in 10 mM phosphate and 10% glycerol buffer (pH:7.2) containing 500 mM NaCl;* ***Lane 5*** *– K134E elution in 10 mM phosphate and 10% glycerol buffer (pH:7.2) containing 800 mM NaCl;* ***Lane 6*** *– FGF1 marker*

The red box indicates the band of interest of K134E

Fluorescence (*Figure 13)* was then run which confirmed proper folding of both the mutant and wild-type protein. For both curves, the peak was around 306 nm.

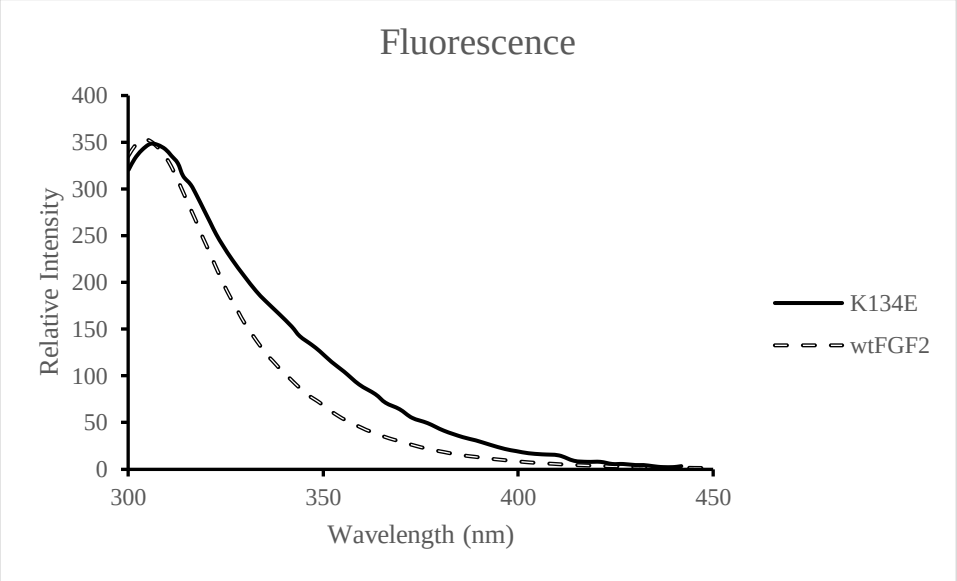

Figure 12: Fluorescence of wtFGF2 (dash) and K134E (solid line) Concentration of protein used was 30 -40 µM in 10 mM phosphate and 10% glycerol buffer (pH:7.2) containing 150 mM NaCl.

DSC (*Figure 14*) was also ran on both samples to verify melting point. The melting point of the wtFGF2 was found to be approximately 37˚C and the melting point of K134E was found to be approximately 51˚C.

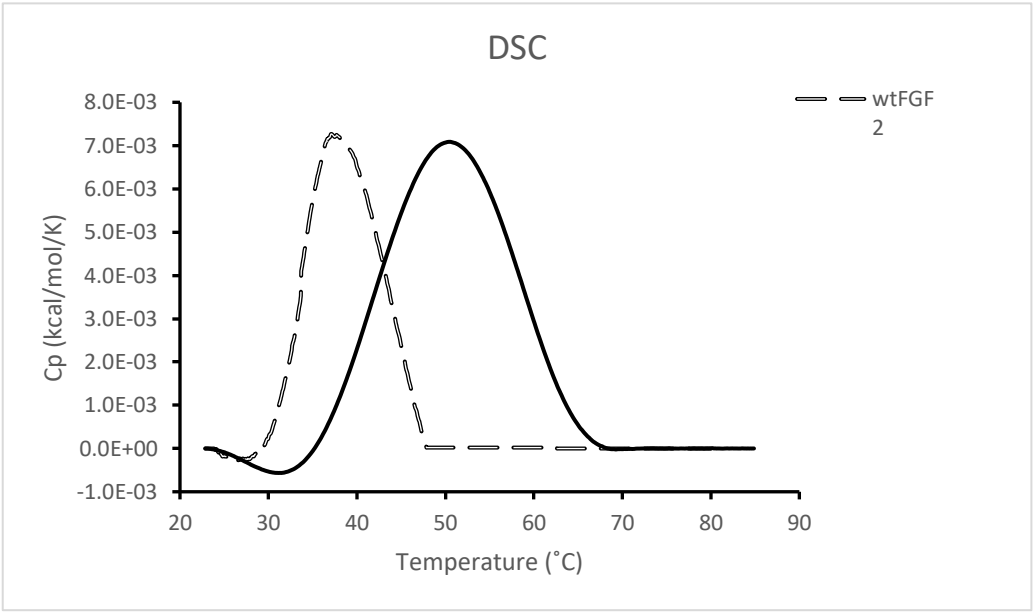

Figure 13:DSC profiles of wt-FGF2 (dash) and the K1343E variant (solid line).

Furthermore, CD was run on the mutant protein to confirm proper folding of the secondary complex of the protein. *Figure 14* confirmed that the mutant protein and wild-type had proper folding and was not aggregated.

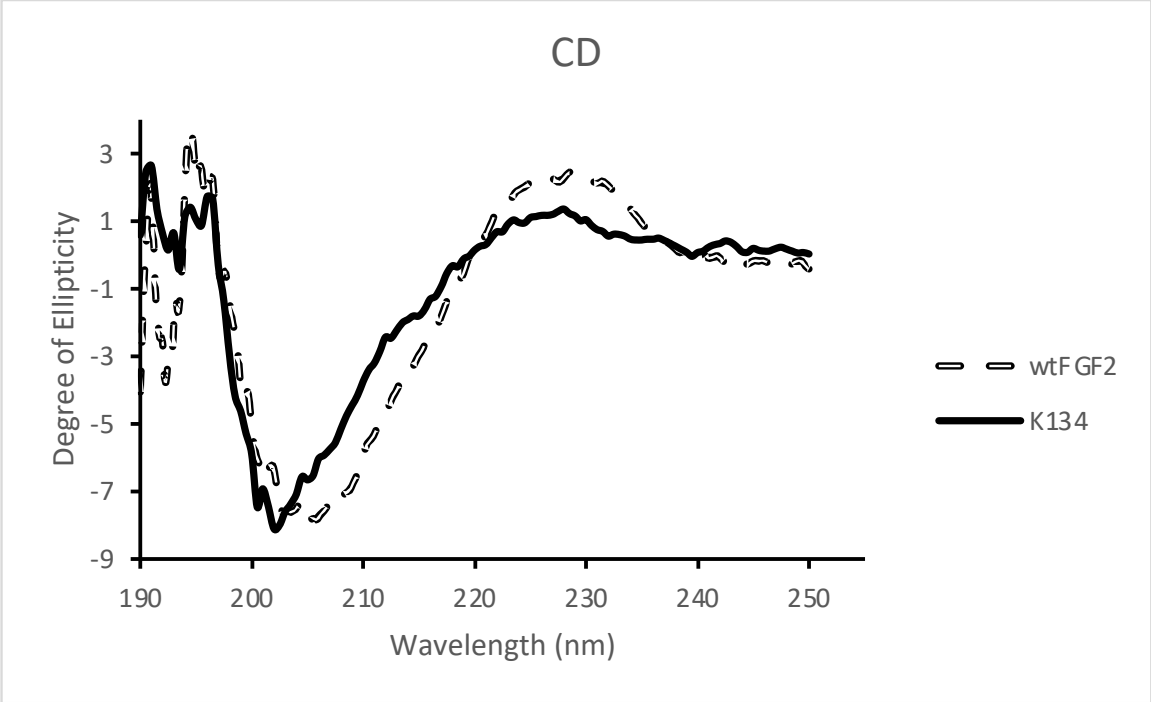

Figure 14: CD was scan on the mutant protein and wild-type protein. Concentration of protein used was 30 -40 µM in 10 mM phosphate and 10% glycerol buffer (pH:7.2) containing 150 mM NaCl

After the first purification on both the mutant and the wild-type, the procedure was modified so that there would be less containment bands when eluting the protein. An additional wash step was added. In this wash step, after the protein was loaded onto the column, a higher concentration salt buffer was run through in hopes of cleaning out the column from any proteins that are desired in the final sample before beginning thrombin cleavage. The salt wash had the same components as Buffer 1 except with increased sodium chloride concentrations. The increased salt concentrations used were 800 mM NaCl and 1500 mM NaCl. The result of these purifications can be seen in *Figure 16.* With increasing salt concertation, there were less contaminant bands in

the both the wild-type and the mutant after performing purification via the GSH-sepharose column.

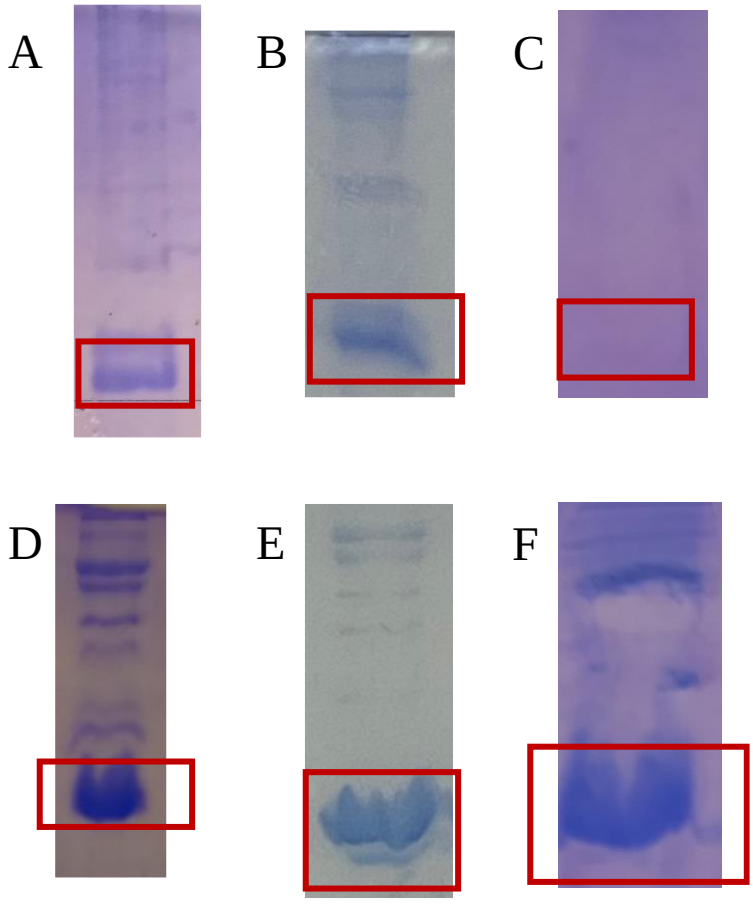

Figure 15: SDS-gel electrophoresis lanes isolated based on presence of FGF2. ***A)*** *K134E elution after no additional salt wash in 10 mM phosphate and 10% glycerol buffer (pH:7.2) containing 150 mM NaCl;* ***B)*** *K134E elution after 10 mM phosphate and 10% glycerol buffer (pH:7.2) containing 800 mM NaCl wash in 10 mM phosphate and 10% glycerol buffer (pH:7.2) containing 150 mM NaCl;* ***C)*** *K134E elution after 10 mM phosphate and 10% glycerol buffer (pH:7.2) containing 1500 mM NaCl wash in 10 mM phosphate and 10% glycerol buffer (pH:7.2) containing 150 mM NaCl;* ***D)*** *wtFGF2elution after no additional salt wash in 10 mM phosphate and 10% glycerol buffer (pH:7.2) containing 150 mM NaCl;* ***E)*** *wtFGF2 after 10 mM phosphate and 10% glycerol buffer (pH:7.2) containing 800 mM NaCl wash in 10 mM phosphate and 10% glycerol buffer (pH:7.2) containing 150 mM NaCl;* ***F))*** *wtFGF2 elution after 10 mM phosphate and 10% glycerol buffer (pH:7.2) containing 1500 mM NaCl wash in 10 mM phosphate and 10% glycerol buffer (pH:7.2) containing 150 mM NaCl*

The red box indicates the band of interest

To ensure proper folding state of the protein, a fluorescence was run on all samples. *Figure 17* shows that the purification using the higher salt concentration resulted in the denaturation of the protein in both the wild-type and the mutant as seen by the fluorescence's peaks shifting significantly right. The peak of properly folded FGF2 was around 306 nm while the peak of the denatured FGF2 varied from 330 – 340 nm.

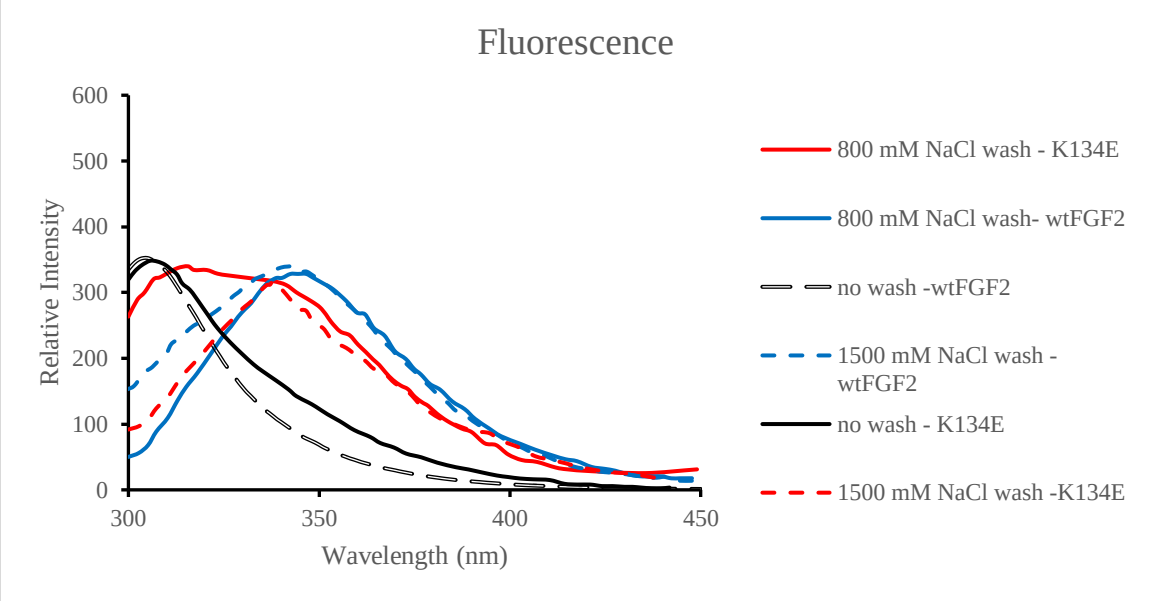

Figure 16: Fluorescence of wtFGF2 no salt-wash (dashed black), K134E no salt wash (solid black), wtFGF2 with 800 mM NaCl wash (solid blue), K134E with 800 mM NaCl wash (solid red), wtFGF2 with 1500 NaCL wash (dashed blue), and K134E with 1500 NaCl wash (dashed red). : Concentration of protein used was 30 -40 µM in 10 mM phosphate and 10% glycerol buffer (pH:7.2) containing 150 mM NaCl

Discussion

The aim of this study was to successfully purify both the both the wild-type and mutant protein and to study the stability of the protein. The results confirmed the proper procedure to purify both the mutant and the wild-type protein was successful. There was at least one successful purification for both proteins. This is seen both by the SDS-PAGE as well as the fluorescence. Previous articles place the peak of florescence of an active FGF2 approximately 305 – 310 nm (22) (23) (24). The peak for wtFGF2 and K134E was approximately 306 nm which confirms its active folded state. Furthermore, the CD confirmed that K134E and wild-type protein had proper folding and proper secondary structure.

The melting temperature of wtFGF2 was found to be approximately 37˚C, while the melting temperature was approximately 51˚C for K134E. This is accurate with previous data acquired by the Kumar lab group which places the melting temperature for the wild-type around 36 - 37 ˚C. This indicates that the mutant had a higher melting point than the wild-type. This indicates that it is likely that the mutant has higher thermal stability than the wild-type. Since a DSC scan was not able to be run with a heparin-wtFGF2 complex or heparin-K134E complex, it is difficult to conclude the degree of thermal stability that K134E has compared to the wtFGF2. Further studies are needed to make a definitive conclusion.

Not all characterization studies listed in the materials and methods could be conducted due to the denaturation of proteins that occurred due to the modification of the purification procedure. The procedure was modified to add the additional salt-washes to hopefully elute a cleaner protein. The protein eluted was cleaner in both the wild-type

and mutant samples as seen in *Figure 16.* The 1500 mM NaCl salt wash resulted in less containment bands than the 800 mM NaCl salt wash. This indicated that the higher the concentration of the salt wash, the cleaner the protein would be eluted. However, all purifications that were conducted with the additional salt-wash resulted in the denaturation of the protein as seen by the fluorescence peaks that are shifted right compared to the active forms of wtFGF2 and K134E as seen in *Figure 17*. The peak of properly folded FGF2 was around 306 nm while the peak of the FGF2 samples that employed the salt wash varied from 330 – 340 nm. Hence, the salt washes failed at improving the procedure since they resulted in denaturation of the protein.

After the purification involving the 800 mM salt wash, there was a ice storm which prevented fluorescence from being run right after purification and it was possible that the power went out during this time. Hence, after this purification, it was unclear if it was a possible power outage or if it was the salt wash that caused the denaturation of the proteins. However, after running the purification with a 1500 mM salt wash and getting similar results, it is logical to assume that it is the salt-wash during the GSH-sepharose purification that caused the denaturation. It is possible that the disulfide bonds between GST-FGF2 lead to increased electrostatic interactions and with the combination of extended exposure to higher salt concentrations it led to possible protein aggregation. Hence, this is why an 800 mM NaCl buffer is able to be used without denaturation of the protein when purifying FGF2 through the heparin-sepharose column because it is lacking the additional disulfide bond that results from the GST-tag.

Both the mutant and the wild-type were successfully eluted at least once. This means to achieve pure FGF2 based on the methodology as produced in the study,

two separate columns must be utilized. The first is a GSH-sepharose column in which GST-FGF2 is purified. After thrombin cleavage, FGF2 can be eluted. However, as shown in the results, this FGF2 is not likely to be pure. Hence, a heparin-sepharose column is needed to be ran on the fractions of FGF2 achieved from the GSH-sepharose column purification to obtain a pure protein without containments.

Conclusion

This study established a proper procedure for the purification of both wtFGF2 and K134E. It is likely that K134E is more thermally stable than wtFGF2. The DSC demonstrated that the melting point of the mutant is higher than the wild-type, but further studies are needed to further support that the thermal stability of K134E is greater than wtFGF2. This would include achieving the melting-point of the wild-type and mutant with heparin and performing thermal denaturation. Furthermore, chemical stability was not able to be assessed due to lack of sufficient protein to perform the required characterization studies.

Future work will include performing remaining characterization studies listed in the materials and methods so that thermal stability and chemical stability can be fully assessed. Furthermore, future work should also involve improving purification procedure such that in the future purer protein is eluted without use of a heparin-sepharose column.

References

1. Uings, I. J.; Farrow, S. N., Cell receptors and cell signalling. *Mol Pathol* **2000,** *53* (6), 295-9.
2. King, M. Growth Factors. https://themedicalbiochemistrypage.org/growth-factors.php#intro
3. Akl, M. R.; Nagpal, P.; Ayoub, N. M.; Tai, B.; Prabhu, S. A.; Capac, C. M.; Gliksman, M.; Goy, A.; Suh, K. S., Molecular and clinical significance of fibroblast growth factor 2 (FGF2 /bFGF) in malignancies of solid and hematological cancers for personalized therapies. *Oncotarget* **2016,** *7* (28), 44735-44762.
4. Yun, Y. R.; Won, J. E.; Jeon, E.; Lee, S.; Kang, W.; Jo, H.; Jang, J.H.; Shin, U. S.; Kim, H. W., Fibroblast growth factors: biology, function, and application for tissue regeneration. *Journal of tissue engineering*, ***2010***, 218142. https://doi.org/10.4061/2010/218142
5. Coughlin, S. R.; Barr, P. J.; Cousens, L. S.; Fretto, L. J.; Williams, L. T., Acidic and basic fibroblast growth factors stimulate tyrosine kinase activity in vivo. *J Biol Chem* **1988,** *263* (2), 993.
6. Beenken, A.; Mohammadi, M., The FGF family: biology, pathophysiology and therapy. *Nat Rev Drug Discov* **2009,** *8* (3), 226. .
7. Schlessinger, J.; Plotnikov, A. N.; Ibrahimi, O. A.; Eliseenkova, A. V.; Yeh, B. K.; Yayon, A.; Linhardt, R. J.; Mohammadi, M., Crystal structure of a ternary FGF-FGFR-heparin complex reveals a dual role for heparin in FGFR binding and dimerization. *Mol Cell* **2000,** *6* (3), 746-50.

8. Ornitz, D. M.; Itoh, N., Fibroblast growth factors. *Genome Biol* **2001,** *2* (3), REVIEWS3005.

9. Paluck, S.J.; Nguyen, T.H.; Lee, J.P.; Maynard, H.D., A Heparin-Mimicking Block Copolymer Both Stabilizes and Increases the Activity of Fibroblast Growth Factor 2 (FGF2). *Biomacromolecules* **2017,** *17*(10), 3386-3395. doi: 10.1021/acs.biomac.6b01182. Epub 2016 Sep 13. PMID: 27580376; PMCID: PMC5059753.

10. Zulueta, M.M.L; Chyan, C.L.; Hung, S.C., Structural analysis of synthetic heparan sulfate oligosaccharides with fibroblast growth factors and heparin-binding hemagglutinin. Curr Opin Struct Biol **2018**, *50*, 126-133. doi: 10.1016/j.sbi.2018.03.003. Epub 2018 Mar 16. PMID: 29554552.

11. Mignatti, P.; Morimoto, T.; Rifkin, D. B., Basic fibroblast growth factor, a protein devoid of secretory signal sequence, is released by cells via a pathway independent of the endoplasmic reticulum-Golgi complex. *J Cell Physiol* **1992,** *151* (1), 81-93.

12. Li, Y.C.; Ho, I.H.; Ku, C.C.; Zhong, Y.Q.; Hu, Y.P.; Chen, Z.G.; Chen, C.Y.; Lin, W.C.; Zulueta, M.M.; Hung, S.C.; Lin, M.G.; Wang, C.C.; Hsiao, C.D. Interactions that influence the binding of synthetic heparan sulfate-based disaccharides to fibroblast growth factor-2. *ACS Chem Biol* **2014**, *9*(8),1712-7. doi: 10.1021/cb500298q. Epub 2014 Jun 26. PMID: 24959968.

13. Mundhenke, C.; Meyer, K.; Drew, S.; Friedl, A., Heparan sulfate proteoglycans as regulators of fibroblast growth factor-2 receptor binding in breast carcinomas. *Am J Pathol*, **2002**,*160*(1):185-194. doi:10.1016/S0002-9440(10)64362-3.

14. Ishihara, M.; Takano, R.; Kanda, T.; Hayashi, K.; Hara, S.; Kikuchi, H.; Yoshida, K., Importance of 6-O-sulfate groups of glucosamine residues in heparin for activation of FGF-1 and FGF-2. *Journal of biochemistry*, **1995,** *118*(6), 1255–1260. https://doi.org/10.1093/oxfordjournals.jbchem.a125015

15. Sperinde, G.V.; Nugent, M.A. ,Mechanisms of fibroblast growth factor 2 intracellular processing: a kinetic analysis of the role of heparan sulfate proteoglycans. *Biochemistry*. **2000**, *39*(13), 3788-96. doi: 10.1021/bi992243d. PMID: 10736179.

16. Frykberg, R.G.; Banks J., Management of Diabetic Foot Ulcers: A Review. *Fed Prac*t **2016,** *33* (2),16-23.

17. Sen, C. K.; Gordillo, G. M.; Roy, S.; Kirsner, R.; Lambert, L.; Hunt, T. K.; Gottrup, F.; Gurtner, G. C.; Longaker, M. T., Human skin wounds: a major and snowballing threat to public health and the economy. *Wound Repair Regen* **2009,** *17* (6), 769-71.

18. Shrestha, L.B; Heisler J.H. *The Changing Demographic Profile of the United States*. Congressional Research Service Library of Congress, **2011.**

19. Han, G.; Ceilley, R., Chronic Wound Healing: A Review of Current Management and Treatments. *Adv Ther* **2017,** *34* (2), 599-610.

20. Benington, L.; Rajan, G.; Locher, C.; Lim, L.Y.., Fibroblast Growth Factor 2—A Review of Stabilization Approaches for Clinical Applications. *Pharmaceutics* **2020**, *12*, 508. https://doi.org/10.3390/pharmaceutics12060508

21. Bush, M. A.; Samara, E.; Whitehouse, M. J.; Yoshizawa, C.; Novicki, D. L.; Pike, M.; Laham, R. J.; Simons, M.; Chronos, N. A., Pharmacokinetics and

pharmacodynamics of recombinant FGF-2 in a phase I trial in coronary artery disease. *J Clin Pharmacol* **2001,** *41* (4), 378-85.

22. Krzyscik, M.; Zakrzewska, M.; Otlewski, J., Site-Specific, Stoichiometric-Controlled, PEGylated Conjugates of Fibroblast Growth Factor 2 (FGF2) with Hydrophilic Auristatin Y for Highly Selective Killing of Cancer Cells Overproducing Fibroblast Growth Factor Receptor 1 (FGFR1). *Molecular Pharmaceutics*, **2020**, *17*. 2734–2748. 10.1021/acs.molpharmaceut.0c00419.
23. Swiderska, K. W.; Szlachcic, A.; Czyrek, A.; Zakrzewska, M.; Otlewski, J., Site-specific conjugation of fibroblast growth factor 2 (FGF2) based on incorporation of alkyne-reactive unnatural amino acid. *Bioorganic and Medicinal Chemistry*, **2017**, *25*(14), 3685–3693. https://doi.org/10.1016/j.bmc.2017.05.003.
24. Krzyscik, M. A.; Zakrzewska, M.; Sørensen, V.; Sokolowska-Wedzina, A.; Lobocki, M.; Swiderska, K. W.; Krowarsch, D.; Wiedlocha, A.; Otlewski, J., Cytotoxic conjugates of fibroblast growth factor 2 (FGF2) with monomethyl auristatin E for effective killing of cells expressing FGF receptors. *ACS Omega*, **2017**, *2*(7), 3792–3805. https://doi.org/10.1021/acsomega.7b00116.